Dystrophin Is a Tumor Suppressor in Human Cancers with Myogenic Programs

Published in final edited form as:
Nat Genet. 2014 June ; 46(6): 601–606. doi:10.1038/ng.2974.

Dystrophin Is a Tumor Suppressor in Human Cancers with Myogenic Programs

Yuexiang Wang[1], **Adrian Marino-Enriquez**[1], **Richard R. Bennett**[2], **Meijun Zhu**[1], **Yiping Shen**[3], **Grant Eilers**[1], **Jen-Chieh Lee**[1], **Joern Henze**[1], **Benjamin S. Fletcher**[1], **Zhizhan Gu**[4], **Edward A. Fox**[5], **Cristina R. Antonescu**[6], **Christopher D.M. Fletcher**[1], **Xiangqian Guo**[7], **Chandrajit P. Raut**[8], **George D. Demetri**[9], **Matt van de Rijn**[7], **Tamas Ordog**[10], **Louis M. Kunkel**[2], and **Jonathan A. Fletcher**[1,*]

[1]Department of Pathology, Brigham and Women's Hospital and Harvard Medical School, Boston, MA, USA

[2]Division of Genetics and Genomics, The Manton Center for Orphan Disease Research, Children's Hospital, Boston, MA, USA

[3]Genetic Diagnostic Laboratory, Department of Laboratory Medicine, Children's Hospital, Boston, MA, USA. & Shanghai Children's Medical Center, Jiaotong University, Shanghai, China

[4]Division of Rheumatology, Immunology, and Allergy, Department of Medicine, Brigham and Women's Hospital and Harvard Medical School, Boston, MA, USA

[5]Molecular Diagnostics Laboratory, Dana-Farber Cancer Institute, Boston, MA, USA

[6]Department of Pathology, Memorial Sloan-Kettering Cancer Center, New York, NY, USA

[7]Department of Pathology, Stanford University Medical Center, Stanford, CA, USA

[8]Department of Surgery, Brigham and Women's Hospital and Harvard Medical School, Boston, MA, USA

[9]Ludwig Center at Dana-Farber Cancer Institute and Harvard Medical School, Department of Medical Oncology, Dana-Farber Cancer Institute, Boston, MA, USA

[10]Center for Individualized Medicine, Enteric Neuroscience Program and Department of Physiology and Biomedical Engineering, Mayo Clinic, Rochester, MN, USA

Abstract

[*]Correspondence to: Jonathan A. Fletcher, M.D., Department of Pathology, Brigham and Women's Hospital, 75 Francis Street, Boston, MA 02115, Phone: 617-732-7883, Fax: 617-278-6921, jfletcher@partners.org.

ACCESSION CODES

NCBI Gene Expression Omnibus (GEO): GSE53021, for genome-wide 250K SNP genotypes of 40 myogenic-cancers and normal controls.

AUTHOR CONTRIBUTIONS

J.A.F. supervised the project. Y.W. and J.A.F. generated the original hypothesis and designed the study. Y.W., A.M.E., R.R.B., M.Z., Y.S., G.E., J.-C.L., J.H., B.S.F., Z.G., Y.S., X. G., and T.O. performed experiments. A.M.E., C.R.A., C.D.M.F., C.P.R., M.v.d.R. and J.A.F. provided samples and clinical data. Y.W., A.M.E., R.R.B., M.Z., Y.S., G.E., J.-C.L., B.S.F., Z.G., E.A.F., X.Q.G., M.v.d.R., T.O., L.M.K. and J.A.F. analyzed data. C.R.A., C.D.M.F., G.D.D., M.v.d.R. and L.M.K. provided scientific advice and helpful comments into the project. Y.W., A.M.E., G.E. and J.A.F. wrote the manuscript. All authors read and approved the final manuscript.

Many common human mesenchymal tumors, including gastrointestinal stromal tumor (GIST), rhabdomyosarcoma (RMS), and leiomyosarcoma (LMS), feature myogenic differentiation[1–3]. Here we report that intragenic deletion of the dystrophin-encoding and muscular dystrophy-associated *DMD* gene is a frequent mechanism by which myogenic tumors progress to high-grade, lethal sarcomas. Dystrophin is expressed in nonneoplastic and benign counterparts for GIST, RMS and LMS, and the *DMD* deletions inactivate larger dystrophin isoforms, including 427kDa dystrophin, while preserving expression of an essential 71kDa isoform. Dystrophin inhibits myogenic sarcoma cell migration, invasion, anchorage independence, and invadopodia formation, and dystrophin inactivation was found in 96%, 100%, and 62% of metastatic GIST, embryonal RMS, and LMS, respectively. These findings validate dystrophin as a tumor suppressor and likely anti-metastatic factor, suggesting that therapies in development for muscular dystrophies may also have relevance in treatment of cancer.

Human cancers featuring myogenic differentiation include LMS, RMS, and GIST. GIST – although most closely resembling interstitial cells of Cajal (ICC) – often express myogenic differentiation markers, such as smooth muscle actin and calponin[4–7]. Presumptive initiating mutations have been identified in these myogenic cancers, including germline *TP53* mutations in patients with LMS and RMS[8,9] and gain-of-function *KIT* or *PDGFRA* mutations in patients with GIST[10–12]. Somatic mutations contribute to tumorigenic progression in myogenic cancers, e.g. cell cycle dysregulation by *CDKN2A* or *TP53* inactivation in GIST[13,14], but few of these genetic progression mechanisms in myogenic cancers have been characterized.

To identify shared tumorigenic mechanisms in myogenic cancers, we performed genome-wide Affymetrix 250K single-nucleotide polymorphism (SNP) assays. These studies revealed intragenic deletions in the Duchenne and Becker muscular dystrophy gene, *DMD*[15] in 25 of 40 high-grade myogenic cancers (63%), including 19 of 29 GISTs, 3 of 4 RMS, and 3 of 7 LMS (Fig. 1a). Although *DMD* is an X-linked gene, the deletions were found in both male and female patients, including 9 of 13 (69%) GISTs in men and 10 of 16 (63%) GISTs in women (Supplementary Table 1). *DMD* deletions in myogenic cancers were not present in companion non-neoplastic tissues, attesting to somatic origin (Fig. 1b). *DMD* deletions, when identified within a primary GIST, were perpetuated in subsequent metastatic lesions (Supplementary Fig. 1), and when identified in any GIST metastasis, were present in other metastases from the same patient (Supplementary Fig. 2). *DMD* intragenic deletions were not detected in 58 non-myogenic sarcomas (Supplementary Table 2) and were observed only infrequently (4.3%) in 905 non-sarcoma human cancer cell lines in the Cancer Cell Line Encyclopedia program[16], (Supplementary Fig. 3). These data show that the frequency of *DMD* deletions is higher in myogenic cancers compared to non-myogenic tumors ($P < 0.0001$).

Whereas all *DMD* deletions in cancers from men were nullizygous, the deletions in cancers from women were either nullizygous (n = 9) or heterozygous (n = 4) (Fig. 2a and Supplementary Table 1). Fluorescence *in situ* hybridization for *DMD* and the Xist inactive X chromosome marker[17] showed that heterozygous *DMD* deletions targeted the active X

chromosome (Fig. 2b). Therefore, both nullizygous and heterozygous *DMD* deletions in female patients caused complete *DMD* inactivation.

DMD is the longest known human gene[15], composed of 79 coding exons spanning 2.2 megabases of the genome, with various transcriptional start sites[18]. Multiplex ligation-dependent probe amplification (MLPA) copy number assessment for each of the *DMD* coding exons revealed intragenic *DMD* deletions in 24 of 56 high-grade myogenic cancers (43%) (Fig. 3, Supplementary Fig. 4 and Supplementary Table 3), all of which were predicted to abrogate expression of the largest dystrophin isoform (427kDa), encoded by *DMD* exons 1–79. By contrast, intragenic *DMD* deletions were not found in 20 benign tumor counterparts for GIST, RMS and LMS (11 low-risk GISTs, 2 rhabdomyomas and 7 leiomyomas), despite high levels of dystrophin expression (Supplementary Table 3). The dystrophin 427kDa isoform was expressed strongly in normal tissue and benign counterparts for GIST, RMS and LMS (Fig. 4), but was undetectable or weakly expressed in 96% of metastatic GISTs (26 of 27), irrespective of whether they contained *KIT* or *PDGFRA* mutations (Fig. 4b and Supplementary Table 4). Similarly, dystrophin 427kDa expression was undetectable or weak in 100% of metastatic embryonal RMS (eRMS) (9 of 9), and 62% of metastatic LMS (8 of 13) (Fig. 4c,d and Supplementary Table 4). Dystrophin 427kDa was also downregulated in 75% of primary “high-risk” GISTs (i.e., GISTs having histologic criteria predictive of metastasis), consistent with the SNP evidence that *DMD* dysregulation is positively selected for in clinically-aggressive primary tumors, even prior to metastasis (Fig. 4b). Expression of 427kDa dystrophin was not detected in 46 non-myogenic sarcomas (Supplementary Table 5). By contrast, expression of dystrophin isoform Dp71 (71kDa), encoded by exons 63–79, is preserved in cancers with *DMD* deletions (Fig. 5). Dp71 is also expressed in non-myogenic sarcomas (Supplementary Fig. 5), in keeping with reports that Dp71 expression is ubiquitous in nonneoplastic tissues, other than skeletal muscle[19]. *DMD Dp71* knockdown in *DMD*-deleted RMS cells inhibited cell growth (Supplementary Fig. 6), indicating that dystrophin 71kDa has essential roles in myogenic cancer cells. These findings account for obligate dystrophin 71kDa expression in myogenic cancers, and explain why *DMD* genomic deletions rarely extend to the coding sequence for this isoform (Fig. 3).

Dystrophin biologic function was evaluated by re-expressing dystrophin in *DMD*-inactivated GIST, RMS and LMS. Re-expression of dystrophin 427kDa is challenging, due to the large size of the cDNA construct. Therefore, we used a *miniDMD* construct lacking exons 17–48 which encode a spectrin-like domain[20] (Fig. 3). This *miniDMD* construct is biologically relevant, inasmuch as it restores crucial aspects of dystrophin function in gene therapy for muscular dystrophy patients[21]. *MiniDMD* transfection into *DMD*-inactivated GIST, eRMS and LMS induced 240kDa dystrophin expression at levels that are physiologic for dystrophin 427kDa expression in low-risk (indolent) GIST, skeletal muscle and myometrium, respectively (Supplementary Fig. 7). Dystrophin re-expression inhibited invasiveness and migration in GIST, eRMS and LMS, but showed no effect in the non-myogenic fibrosarcoma cell line HT-1080 (Fig. 6a,b), and reduced the number of viable cells in eRMS and LMS, but not in GIST, fibrosarcoma, Ewing’s sarcoma or HEK 293 cells (Supplementary Fig. 8). Dystrophin re-expression inhibited anchorage-independent growth in *DMD*-inactivated GIST, eRMS and LMS (Fig. 7a), but not in comparator non-myogenic

fibrosarcoma or Ewing's sarcoma (Fig. 7a and Supplementary Fig. 9). These studies support the hypothesis that *DMD* inactivation enhances metastatic potential selectively in cancers with myogenic programs.

Dystrophin provides a structural link between the actin-based cytoskeleton and extracellular matrix[22,23], which is consistent with our evidence that dystrophin regulates invasion and migration in myogenic cancers. Metastases account for 90% of cancer-related deaths[24,25], and some invasive cancer cells feature invadopodia, which are actin-rich membrane protrusions regulating metastatic behavior[26]. Restoration of *DMD* expression inhibited invadopodia formation in GIST and LMS (Fig. 7b), also consistent with dystrophin function as an anti-metastatic factor.

The genomic, clinicopathological and functional evidence herein demonstrate dystrophin tumor suppressor roles contributing to permissiveness for metastatic behavior in human cancers. The relevance of these findings is supported by reports of spontaneous RMS in *DMD*-inactivated *mdx* mice[27–29]. Similarly, reports of RMS in Duchenne muscular dystrophy patients suggest that germline *DMD* inactivation may predispose to myogenic cancer[30,31]. *DMD* is a large gene, but of the >40 human genes that are more than 1 megabase in genomic length, only *DMD* is known to have frequent deletions that seem subject to strong selective pressure in pre-metastatic GIST. Several observations support *DMD* inactivation as a driver event in myogenic cancers: 1) frequent *DMD* deletions are not found in non-myogenic cancers (Supplementary Fig. 3), most of which have more complex genomic landscapes than those in RMS and GIST[32], indicating that clonal *DMD* deletions in advanced myogenic cancers are not attributable merely to cytogenomic complexity; 2) *DMD* deletions are not found in benign precursors to GIST (Fig. 4b) but rather are remarkably frequent late events in GIST progression and are found in subclones which – based on the genomic evidence – overgrow *DMD*-wildtype subclones in the same tumors; 3) although a late event in tumorigenesis, the same *DMD* deletion found in one metastasis can be detected in all other metastases from the patient (Supplementary Fig. 2), consistent with a biologic advantage for dystrophin inactivation. These genomic lines of evidence, coupled with demonstration that *DMD*-restoration is only impactful in myogenic cancers (Fig. 6,7), suggests that *DMD* mutations in myogenic cancers are classic tumor suppressor events.

It is unclear whether the *DMD* mutation rate is particularly high in myogenic cancers, perhaps due to mechanisms such as transcription-associated recombination[33], but in any case the combined evidence summarized above suggests that *DMD* inactivation may be more than simply a passenger event in myogenic cancer. Previously, *DMD* deletions were demonstrated in 5.5% of malignant melanoma[34], but it is unknown whether those deletions had functional consequences. In clinically-advanced myogenic cancers, we show that *DMD* inactivation abolishes the dystrophin 427kDa expression found in normal tissue and benign counterparts for GIST, LMS and RMS, while preserving dystrophin 71kDa protein, which appears to be an obligate factor in these cancers. Dystrophin interacts with a complex of sarcolemmal proteins and glycoproteins known as dystrophin-associated proteins[22], and our demonstration of dystrophin tumor suppressor roles anticipates that other proteins in this complex might regulate tumorigenic functions. As one example, the dystrophin-related protein, utrophin, is a potential tumor suppressor in non-myogenic malignancies[35], and

pharmacologic induction of utrophin overexpression in *mdx* mice prevents development of muscular dystrophy, suggesting that utrophin can compensate for dystrophin deficiency[36]. Other treatment options to correct dystrophin defects are undergoing evaluation in clinical trials for Duchenne muscular dystrophy[37–40], and these approaches warrant evaluation as potential therapeutic agents in oncology. Identification of patients whose cancers have dystrophin defects might be expedited by immunohistochemical screening for loss of dystrophin 427kDa expression. Immunohistochemical assays show robust dystrophin expression in nonneoplastic myogenic cells (skeletal, cardiac, and smooth muscle) and in leiomyoma (benign smooth muscle tumors) (Supplementary Fig. 10a,c), whereas LMS (malignant smooth muscle tumors) often feature complete loss of demonstrable dystrophin expression (Supplementary Fig. 10b,c). Therefore, dystrophin dysregulation warrants evaluation as a prognostic factor in myogenic cancers, and as a potential point of therapeutic attack.

METHODS

Tumor and tissue samples

Snap-frozen tumor biopsies and matched normal tissue samples were from patients at Brigham and Women's Hospital and Memorial Sloan Kettering Cancer Center. All samples were collected with institutional review board approval.

SNP arrays

High molecular weight genomic DNA was isolated using QIAamp DNA Mini Kit (QIAGEN) and analyzed by Affymetrix 250K SNP array. DNA was digested with *Nsp*1, and linkers were ligated to the restriction fragments to permit PCR amplification. The PCR products were purified and fragmented by treatment with DNase I, then labeled and hybridized to microarray chips. The positions and intensities of the fluorescence emissions were analyzed using dChip software. Array intensity was normalized to the array with median intensity. Median smoothing was used to infer copy number.

Fluorescence *in situ* hybridization and *Xist* evaluation

BACs RP11-42E12 (*DMD*, chromosome Xp21.1; start position 32,642,966 GRCh37/hg19; end position 32,848,014; targeting *DMD* introns 4–9) and RP11-939O17 (*DMD*, chromosome Xp21.1; start position 32,844,043; end position 33,018,177; targeting *DMD* introns 2–4) were obtained from BAC/PAC Resources (Children's Hospital, Oakland, CA). BAC DNA was labeled using a nick translation kit with Spectrum Orange-11-dUTP (*DMD*). As a control for X chromosome copy number a centromere X probe (DXZ1, spectrum aqua probe) was obtained from Abbott Laboratories (Vysis, Abbott Park, Illinois). A fosmid clone overlapping the *Xist* locus (G248P8779H11; Xq13.2; start position 73,038,817; end position 73,075,707) was obtained from BAC/PAC Resources (Children's Hospital, Oakland, CA). The fosmid DNA was labeled by nick translation with Spectrum Green-11-dUTP, and used in a triple-hybridization with the probes for *DMD* (spectrum orange) and centromere X (aqua) according to standard protocols.

Multiplex Ligation-dependent Probe Amplification (MLPA)

The MLPA procedure and capillary electrophoresis were performed using SALSA MLPA kits P034-A2 and P035-A2 from MRC-Holland. The combined P034 and P035 kits contain probes for each of the 79 *DMD* coding exons and for the alternative exon 1 Dp427c. MLPA reactions were conducted using a G-Storm GS1 thermal cycler (Gene Technologies Ltd) with fragment analysis by ABI-3130XL Genetic Analyzer and GeneMapper software (Applied Biosystems). Raw data were received as peak heights, as a measure of peak intensity, for each of the probes.

Purification of murine interstitial cells of Cajal (ICC)

Murine ICC (~500,000) were isolated as $Kit^{+}CD44^{+}CD34^{-}$ cells from the hematopoietic marker-negative ($CD45^{-}F4/80^{-}CD11b^{-}$) fraction of the gastric tunica muscularis of day 7–15 BALB/c mice (n = 52, in 5 cohorts) as described previously[41,42]. The fidelity of ICC sorting was validated by demonstrating a >2.5-fold increase in KIT protein expression in sorted compared to unsorted cells and by lack of expression of the smooth muscle marker Myh11 and the pan-neural marker PGP 9.5 by western blotting.

Western blotting

Frozen tumor samples were diced in ice-cold lysis buffer (1% NP-40, 50 mM Tris-HCl pH 8.0, 100 mM sodium fluoride, 30 mM sodium pyrophosphate, 2 mM sodium molybdate, 5 mM EDTA, 2 mM sodium orthovanadate) on dry ice and homogenized with a Tissue Tearor Homogenizer for 3 seconds, 3–5 times, on ice, and the cell lysate was then rocked overnight at 4°C. Lysates were cleared by centrifugation at 14,000 rpm for 30 min at 4°C, and lysate protein concentrations were determined using a Bio-Rad protein assay (Bio-Rad Laboratories Hercules, CA, USA). Electrophoresis and western blotting were performed using standard techniques. The hybridization signals were detected by chemiluminescence (Immobilon Western, Millipore Corporation, MA) and captured using a FUJI LAS1000-plus chemiluminescence imaging system (Fuji Film, Tokyo, Japan). Primary antibodies were DYS1 (Novocastra, NCL-DYS1, raised against the dystrophin rod domain, amino acids 1181 and 1388, detects 427 kDa dystrophin isoform), DYS2 (Novocastra, NCL-DYS2, raised against the C-terminal 17 amino acids of dystrophin, detects 240 kDa mini-dystrophin), 7A10 (Santa Cruz, sc-47760, raised against amino acids 3200–3684 of dystrophin, detects Dp71), and GAPDH (Sigma, G8795).

Cell lines

GIST-T1 was generously provided by Dr. Takahiro Taguchi[43]. HT-1080 and HEK 293 were obtained from the American Type Culture Collection. All other cell lines were developed in the Jonathan Fletcher laboratory at Brigham and Women's Hospital. GIST-T1 and GIST430 were established from metastatic GISTs with *DMD* exon 1 and exons 1–9 deletions, respectively. RMS176 was established from a metastatic eRMS with *DMD* exons 1–7 and exons 21–44 deletions. LMS04 was established from a metastatic LMS without apparent *DMD* deletion but with complete loss of 427kDa dystrophin expression. The HT-1080 fibrosarcoma[44] and EWS502 Ewing's sarcoma were non-myogenic controls with wildtype *DMD*.

Stable transfections

GIST-T1, GIST430, RMS176, LMS04 and EWS502 cell monolayers were disaggregated with trypsin and resuspended in Amaxa Nucleofector solution V (Amaxa Biosystems) at a concentration of 1×10^6 cells per 100 μl. Nucleofection was performed using program T-030 on a Nucleofector II machine (Amaxa Biosystems). One microgram of pCR3.1-EGFP or pCR3.1-*miniDMD* plasmid was used for electroporation. Transfected cells were selected with G418 for 5 days before analyses.

Dp71 siRNA knockdown

Dp71-specific siRNA, targeting the unique region in exon 1 of *Dp71*, was obtained from Invitrogen (sequence provided in Supplementary Table 6). Control siRNA was obtained from Invitrogen (Stealth RNAi™ siRNA negative control medium GC Duplex, Catalog # 12935-300). siRNA was delivered into RMS176 and RMS843 cells by nucleofection (Amaxa Biosystems) as described previously[45].

Cell viability assays

Viability studies were performed using the CellTiter-Glo luminescent assay (Promega, Madison, WI). Cells were plated at 2,000 cells per well in a 96-well flat-bottomed plate (Falcon, Lincoln, NJ). Luminescence was analyzed using a Veritas microplate luminometer (Turner Biosystems, Sunnyvale, CA).

Soft agar assay

Cells were plated in 35mm dishes after stable transfection of *EGFP* or *miniDMD*. The cells were incubated for 3–4 weeks and then stained with 1 ml of 1 mg/ml methyl thiazol tetrazolium (MTT) for 3 hours. Colonies were counted manually. All experiments were performed in triplicate.

Quantitative cell invasion and migration assays

0.3 ml serum free media containing 0.3×10^5 GIST-T1, GIST430, RMS176 or LMS04 cells were plated for invasion assays in BD BioCoat™ Matrigel Invasion Chambers (BD Biosciences, Catalog # 354480) and for migration assays in BD BioCoat™ 8.0 μm PET Membrane 24-well Cell Culture Inserts (BD Biosciences, Catalog # 354578). The wells were fed with 0.5ml RPMI Media 1640 (Invitrogen) containing 15% FBS and incubated in a humidified incubator, at 37°C, 5% CO_2 for 144 hours (GIST-T1), 72 hours (GIST430) or 24 hours (RMS176, LMS04, and HT-1080). The media from the inside of the insert was aspirated, and the interiors of the inserts were gently swabbed to remove non-invasive or non-migratory cells. Inserts were transferred to new wells containing 400 μl Cell Stain Solution (Cell Biolabs, Inc) and incubated for 10 minutes at room temperature, then rinsed two times in a beaker of water. Then, the inserts were air dried and transferred to new wells containing 200 μl Extraction Solution (Cell Biolabs, Inc) and quantified at OD 560nm in a microplate reader.

Radius 2-D cell migration assay

Impact of dystrophin restoration on cell migration was determined using a 2-dimensional gap closure radius 24-well migration assay, according to the manufacturer's instructions (Cell Biolabs, Inc).

Immunofluorescence

5×10^4 cells were plated on 10-mm glass coverslips coated with 1 μg/cm^2 fibronectin (Sigma-Aldrich). Cells were fixed in 4% paraformaldehyde (Electron Microscopy Sciences) for 15 min, permeabilized for 10 min. with 0.3% Triton X-100 (Thermo Fisher Scientific) for 10 min, incubated with primary antibodies overnight at 4°C, then with secondary antibody for 1 hour, and mounted on slides with FluorSave™ reagent (EMD Millipore Chemicals). Cells were stained for cortactin and MMP14 to identify invadopodia.

Immunohistochemistry

Immunohistochemistry was performed on tissue and tumor sections using DYS1 mouse monoclonal antibody (Novocastra, NCL-DYS1). Four micron slides were deparaffinized in xylene and hydrated in a graded series of alcohol. The deparaffinized slides were then boiled by microwave for 12 minutes in citrate buffer (pH 6). The IHC reactions were visualized by diaminobenzidine staining, using an EnVision+ system (Dako, Carpinteria, CA, USA).

Statistical analysis

Two-tailed unpaired t-tests were performed for comparison of means analysis. For 2×2 contingency tables, two-tailed P values were calculated using Fisher's exact test.

Supplementary Material

Refer to Web version on PubMed Central for supplementary material.

Acknowledgments

We thank J. Tremblay for the pCR3.1-*miniDMD* construct, T. Taguchi for the GIST-T1 cell line, M. Bardsley and H. Qiu for expert technical assistance. This work was supported by grants from GI SPORE 1P50CA12703-05 (J.A.F., G.D.D.), the Virginia and Daniel K. Ludwig Trust for Cancer Research (J.A.F., G.D.D.), 5R01DK058185-11 (T.O.), GIST Cancer Research Fund (J.A.F.), the Life Raft Group (J.A.F., T.O., M.v.d.R.), Cesarini Pan Mass Challenge for GIST (J.A.F., G.D.D.), Paul's Posse of the Pan Mass Challenge (J.A.F., G.D.D.), the Bernard F. and Alva B. Gimbel Foundation (L.M.K.), and Sarcoma Alliance for Research Through Collaboration (A.M.E.).

References

1. Corless CL, Barnett CM, Heinrich MC. Gastrointestinal stromal tumours: origin and molecular oncology. Nat Rev Cancer. 2011; 11:865–878. [PubMed: 22089421]
2. Arndt CA, Crist WM. Common musculoskeletal tumors of childhood and adolescence. N Engl J Med. 1999; 341:342–352. [PubMed: 10423470]
3. Hernando E, et al. The AKT-mTOR pathway plays a critical role in the development of leiomyosarcomas. Nat Med. 2007; 13:748–753. [PubMed: 17496901]
4. Corless CL, Fletcher JA, Heinrich MC. Biology of gastrointestinal stromal tumors. J Clin Oncol. 2004; 22:3813–3825. [PubMed: 15365079]

5. Taylor BS, et al. Advances in sarcoma genomics and new therapeutic targets. Nat Rev Cancer. 2011; 11:541–557. [PubMed: 21753790]
6. Hettmer S, Wagers AJ. Muscling in: Uncovering the origins of rhabdomyosarcoma. Nat Med. 2010; 16:171–173. [PubMed: 20134473]
7. Edris B, et al. Antibody therapy targeting the CD47 protein is effective in a model of aggressive metastatic leiomyosarcoma. Proc Natl Acad Sci USA. 2012; 109:6656–6661. [PubMed: 22451919]
8. Würl P, et al. Frequent occurrence of p53 mutations in rhabdomyosarcoma and leiomyosarcoma, but not in fibrosarcoma and malignant neural tumors. Int J Cancer. 1996; 69:317–323. [PubMed: 8797875]
9. Ognjanovic S, Olivier M, Bergemann TL, Hainaut P. Sarcomas in TP53 germline mutation carriers: a review of the IARC TP53 database. Cancer. 2012; 118:1387–1396. [PubMed: 21837677]
10. Hirota S, et al. Gain-of-function mutations of c-kit in human gastrointestinal stromal tumors. Science. 1998; 279:577–580. [PubMed: 9438854]
11. Heinrich MC, et al. PDGFRA activating mutations in gastrointestinal stromal tumors. Science. 2003; 299:708–710. [PubMed: 12522257]
12. Rossi S, et al. Molecular and clinicopathologic characterization of gastrointestinal stromal tumors (GISTs) of small size. Am J Surg Pathol. 2010; 34:1480–1491. [PubMed: 20861712]
13. Schneider-Stock R, et al. Loss of p16 protein defines high-risk patients with gastrointestinal stromal tumors: a tissue microarray study. Clin Cancer Res. 2005; 11:638–645. [PubMed: 15701851]
14. Henze J, et al. p53 modulation as a therapeutic strategy in gastrointestinal stromal tumors. PLoS One. 2012; 7:e37776. [PubMed: 22662219]
15. Hoffman EP, Brown RH Jr, Kunkel LM. Dystrophin: the protein product of the Duchenne muscular dystrophy locus. Cell. 1987; 51:919–928. [PubMed: 3319190]
16. Barretina J, et al. The Cancer Cell Line Encyclopedia enables predictive modelling of anticancer drug sensitivity. Nature. 2012; 483:603–607. [PubMed: 22460905]
17. Duszczyk MM, Wutz A, Rybin V, Sattler M. The Xist RNA A-repeat comprises a novel AUCG tetraloop fold and a platform for multimerization. RNA. 2011; 17:1973–1982. [PubMed: 21947263]
18. Muntoni F, Torelli S, Ferlini A. Dystrophin and mutations: one gene, several proteins, multiple phenotypes. Lancet Neurol. 2003; 2:731–40. [PubMed: 14636778]
19. Tadayoni R, Rendon A, Soria-Jasso LE, Cisneros B. Dystrophin Dp71: the smallest but multifunctional product of the Duchenne muscular dystrophy gene. Mol Neurobiol. 2012; 45:43–60. [PubMed: 22105192]
20. Chapdelaine P, et al. Functional EGFP-dystrophin fusion proteins for gene therapy vector development. Protein Eng. 2000; 13:611–615. [PubMed: 11054455]
21. Tang Y, Cummins J, Huard J, Wang B. AAV-directed muscular dystrophy gene therapy. Expert Opin Biol Ther. 2010; 10:395–408. [PubMed: 20132060]
22. Ervasti JM, Campbell KP. Membrane organization of the dystrophin-glycoprotein complex. Cell. 1991; 66:1121–1131. [PubMed: 1913804]
23. Berk BC, Fujiwara K, Lehoux S. ECM remodeling in hypertensive heart disease. J Clin Invest. 2007; 117:568–575. [PubMed: 17332884]
24. Valastyan S, Weinberg RA. Tumor metastasis: molecular insights and evolving paradigms. Cell. 2011; 147:275–292. [PubMed: 22000009]
25. Hanahan D, Weinberg RA. Hallmarks of cancer: the next generation. Cell. 2011; 144:646–674. [PubMed: 21376230]
26. Murphy DA, Courtneidge SA. The ‘ins’ and ‘outs’ of podosomes and invadopodia: characteristics, formation and function. Nat Rev Mol Cell Biol. 2011; 12:413–426. [PubMed: 21697900]
27. Fernandez K, Serinagaoglu Y, Hammond S, Martin LT, Martin PT. Mice lacking dystrophin or alpha sarcoglycan spontaneously develop embryonal rhabdomyosarcoma with cancer-associated p53 mutations and alternatively spliced or mutant Mdm2 transcripts. Am J Pathol. 2010; 176:416–434. [PubMed: 20019182]

28. Chamberlain JS, Metzger J, Reyes M, Townsend D, Faulkner JA. Dystrophin-deficient mdx mice display a reduced life span and are susceptible to spontaneous rhabdomyosarcoma. FASEB J. 2007; 21:2195–2204. [PubMed: 17360850]
29. Schmidt WM, et al. DNA damage, somatic aneuploidy, and malignant sarcoma susceptibility in muscular dystrophies. PLoS Genet. 2011; 7:e1002042. [PubMed: 21533183]
30. Rossbach HC, Lacson A, Grana NH, Barbosa JL. Duchenne muscular dystrophy and concomitant metastatic alveolar rhabdomyosarcoma. J Pediatr Hematol Oncol. 1999; 21:528–530. [PubMed: 10598666]
31. Jakab Z, Szegedi I, Balogh E, Kiss C, Oláh E. Duchenne muscular dystrophy-rhabdomyosarcoma, ichthyosis vulgaris/acute monoblastic leukemia: association of rare genetic disorders and childhood malignant diseases. Med Pediatr Oncol. 2002; 39:66–68. [PubMed: 12116087]
32. Barretina J, et al. Subtype-specific genomic alterations define new targets for soft-tissue sarcoma therapy. Nat Genet. 2010; 42:715–721. [PubMed: 20601955]
33. Gottipati P, et al. Transcription-associated recombination is dependent on replication in Mammalian cells. Mol Cell Biol. 2008; 28:154–164. [PubMed: 17967877]
34. Körner H, et al. Digital karyotyping reveals frequent inactivation of the dystrophin/DMD gene in malignant melanoma. Cell Cycle. 2007; 6:189–198. [PubMed: 17314512]
35. Li Y, et al. UTRN on chromosome 6q24 is mutated in multiple tumors. Oncogene. 2007; 26:6220–6228. [PubMed: 17384672]
36. Tinsley JM, et al. Daily treatment with SMTC1100, a novel small molecule utrophin upregulator, dramatically reduces the dystrophic symptoms in the mdx mouse. PLoS One. 2011; 6:e19189. [PubMed: 21573153]
37. Cirak S, et al. Exon skipping and dystrophin restoration in patients with Duchenne muscular dystrophy after systemic phosphorodiamidate morpholino oligomer treatment: an open-label, phase 2, dose-escalation study. Lancet. 2011; 378:595–605. [PubMed: 21784508]
38. Kawahara G, et al. Drug screening in a zebrafish model of Duchenne muscular dystrophy. Proc Natl Acad Sci USA. 2011; 108:5331–5336. [PubMed: 21402949]
39. Gehrig SM, et al. Hsp72 preserves muscle function and slows progression of severe muscular dystrophy. Nature. 2012; 484:394–398. [PubMed: 22495301]
40. Seto JT, Ramos JN, Muir L, Chamberlain JS, Odom GL. Gene Replacement Therapies for Duchenne Muscular Dystrophy Using Adeno-Associated Viral Vectors. Curr Gene Ther. 2012; 12:139–151. [PubMed: 22533379]
41. Bardsley MR, et al. Kit^{low} stem cells cause resistance to Kit/platelet-derived growth factor α inhibitors in murine gastrointestinal stromal tumors. Gastroenterology. 2010; 139:942–952. [PubMed: 20621681]
42. Izbeki F, et al. Loss of Kit^{low} progenitors, reduced stem cell factor and high oxidative stress underlie gastric dysfunction in progeric mice. J Physiol. 2010; 588:3101–3117. [PubMed: 20581042]
43. Taguchi T, et al. Conventional and molecular cytogenetic characterization of a new human cell line, GIST-T1, established from gastrointestinal stromal tumor. Lab Invest. 2002; 82:663–665. [PubMed: 12004007]
44. Rasheed S, Nelson-Rees WA, Toth EM, Arnstein P, Gardner MB. Characterization of a newly derived human sarcoma cell line (HT-1080). Cancer. 1974; 33:1027–1033. [PubMed: 4132053]
45. Patial S, Luo J, Porter KJ, Benovic JL, Parameswaran N. G-protein-coupled-receptor kinases mediate TNFα-induced NFκB signalling via direct interaction with and phosphorylation of IκBα. Biochem J. 2009; 425:169–178. [PubMed: 19796012]

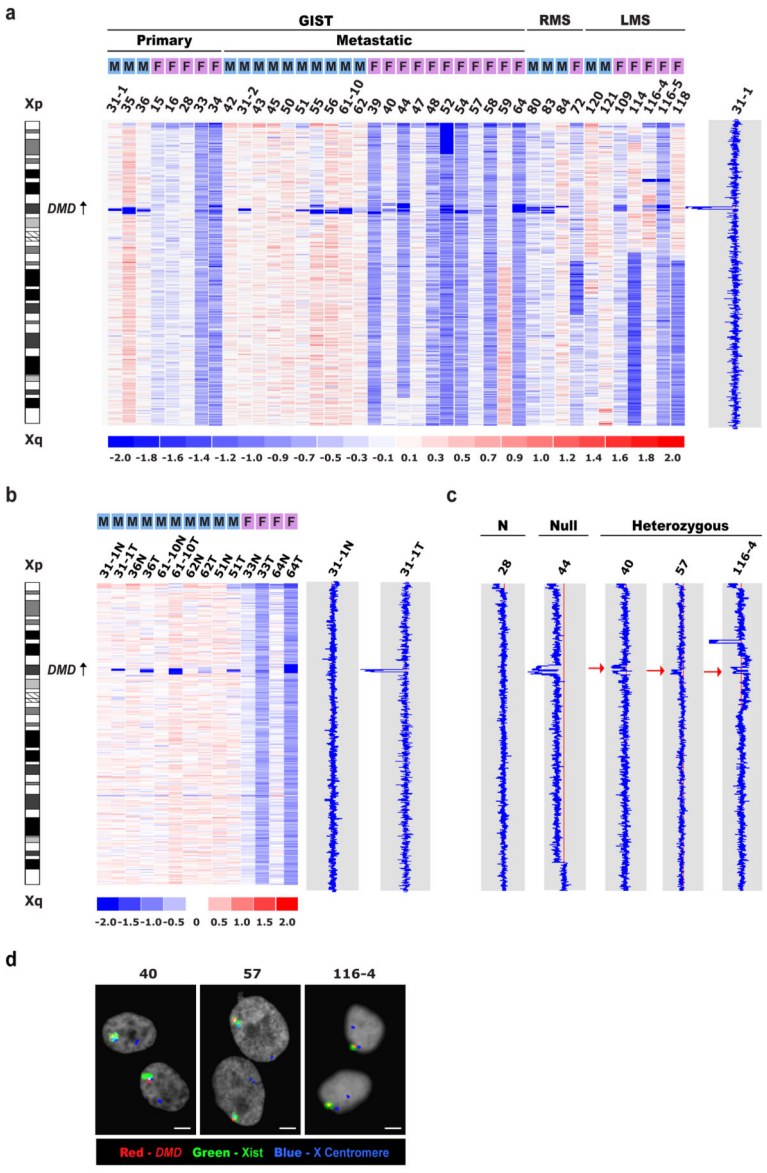

Figure 1.

Identification of somatic intragenic *DMD* deletions in human myogenic cancers. (**a**) dChip SNP log2 ratio copy number evaluations demonstrate intragenic *DMD* deletions in 25 of 40 (63%) primary or metastatic myogenic cancers. M denotes male and F denotes female (full clinicopathological details are provided in Supplementary Table 1). Panel on right depicts representative SNP profile with *DMD* deletion in GIST from a male patient. (**b**) SNP evaluations in matched cancer and non-neoplastic cell DNAs from the same patients, demonstrating tumor-restricted nature of *DMD* deletions. (**c** and **d**) *DMD* deletions in myogenic cancers from women. (**c**) dChip SNP analyses showing normal *DMD* copy number (N, case 28), nullizygous *DMD* deletion (Null, case 44) and heterozygous *DMD* deletions (cases 40 and 57 are metastatic GISTs; case 116-4 is metastatic LMS). (**d**) FISH and Xist analysis in cases 40, 57, and 116-4, showing *DMD* deletion in the Xist-negative

active X chromosome. Probes are for *DMD* (red), X centromere (blue), and Xist (green). Scale bars, 2 μm.

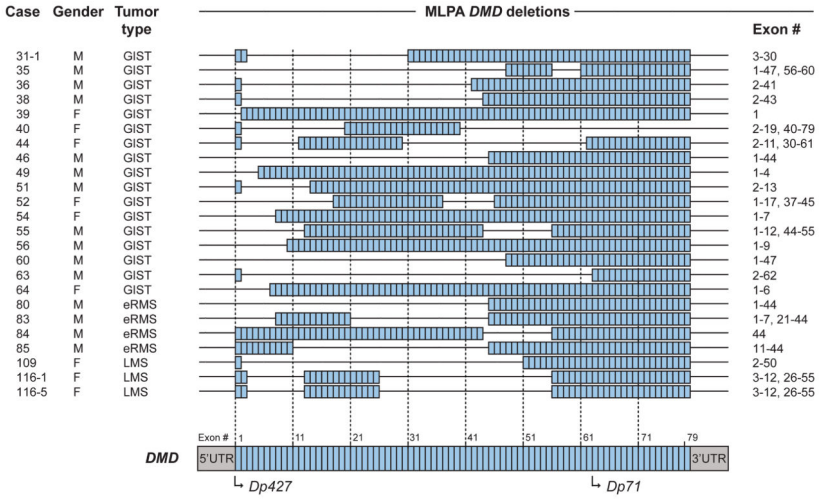

Figure 2.

MLPA evaluations of *DMD* exons 1–79 show intragenic deletions in 24 myogenic cancers.

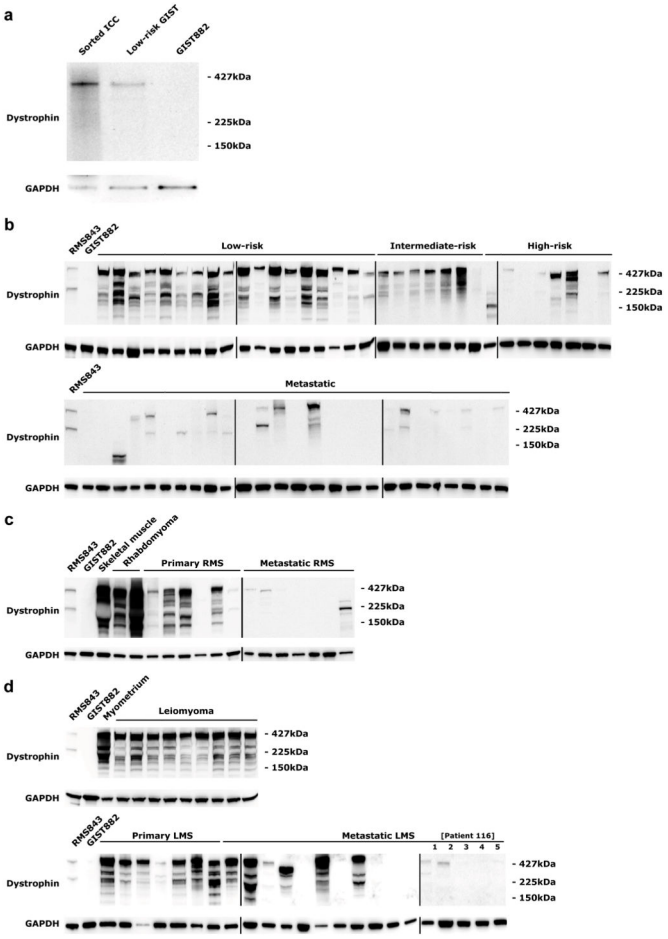

Figure 3.

Loss of dystrophin 427kDa expression in most metastatic GIST, RMS and LMS. Western blotting with DYS1 demonstrates dystrophin expression in the normal tissue and benign tumor counterparts for GIST, RMS and LMS (**a** to **d**); low-risk GIST is a clinically indolent precursor to malignant GIST. Loss of dystrophin 427kDa expression is demonstrated in most metastatic GIST (**b**), RMS (**c**) and LMS (**d**). Patient 116 samples (**d**) are five successive LMS metastases, resected during an 8 year interval in the same patient.

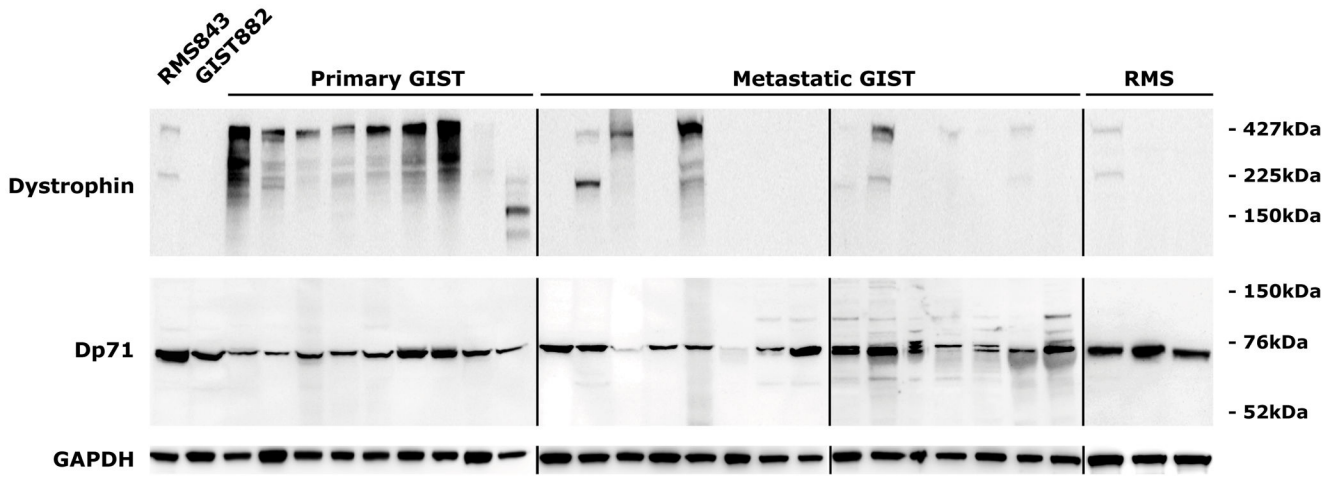

Figure 4.

Expression of Dp71 dystrophin in myogenic tumors. Western blotting with dystrophin antibody 7A10 demonstrates Dp71 expression in primary GIST, metastatic GIST, and RMS cases, including those with loss of 427kDa dystrophin.

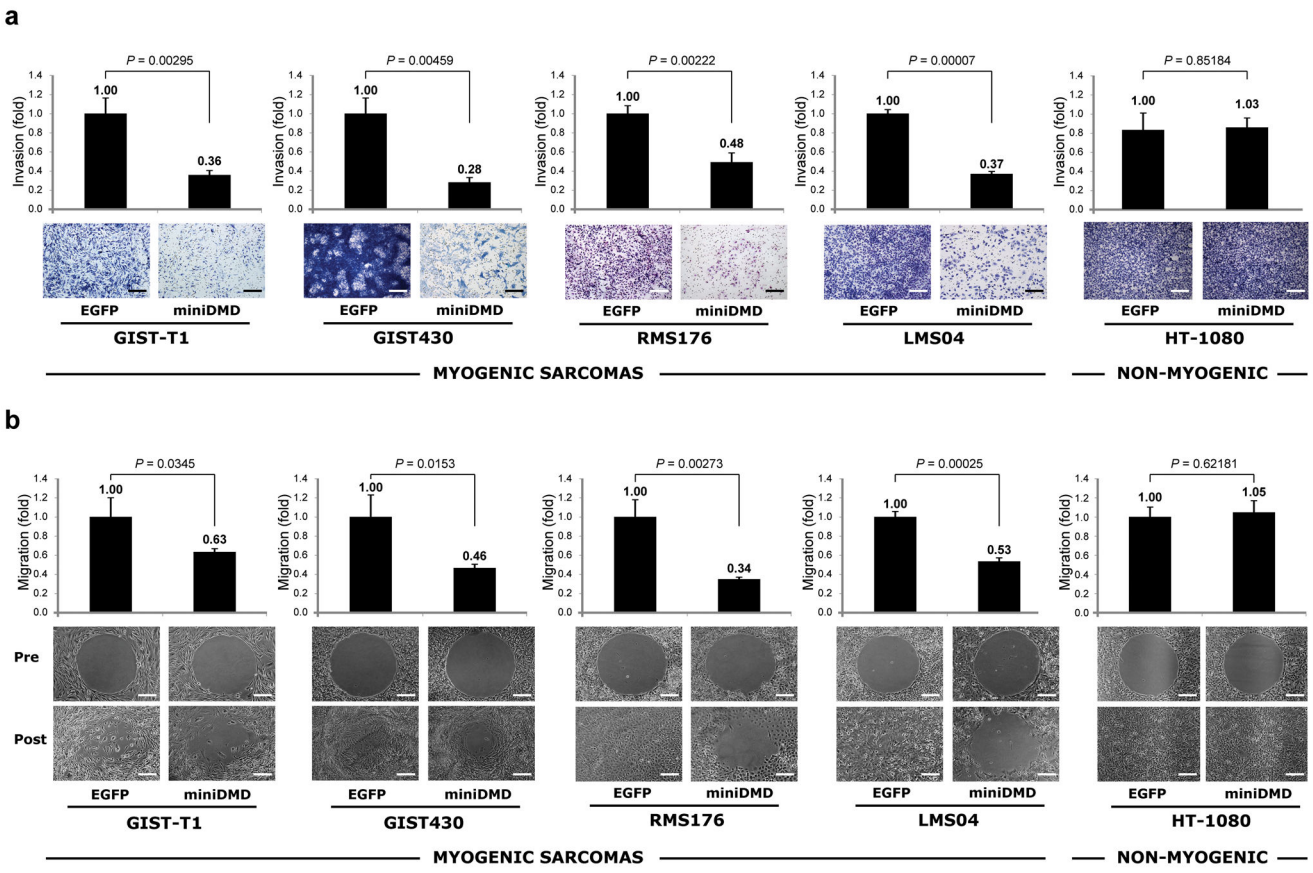

Figure 5.

Restoration of dystrophin expression inhibits invasiveness and migration in *DMD*-inactivated GIST, RMS and LMS, but not in a comparator non-myogenic fibrosarcoma (HT-1080). Three biological replicates of each experiment were evaluated; the error bars on the histograms indicate standard deviation of the mean. Scale bars, 100 μm. (**a**) *miniDMD* restoration in GIST, RMS and LMS inhibits invasion in Matrigel assays. GIST, RMS, LMS and fibrosarcoma cells were seeded and invasion toward 15% FBS was measured after 144 hours (GIST) or 24 hours (RMS, LMS and fibrosarcoma). Cells invading to the bottom of the membrane were stained and quantified at OD 560nm after extraction. (**b**) *miniDMD* restoration in GIST, RMS and LMS, but not in HT-1080 fibrosarcoma, inhibits migration, as assessed by Radius 2-D cell migration assay and by a complementary assay of migration toward 15% FBS on a polycarbonate membrane: migration was quantified at OD 560nm after extraction.

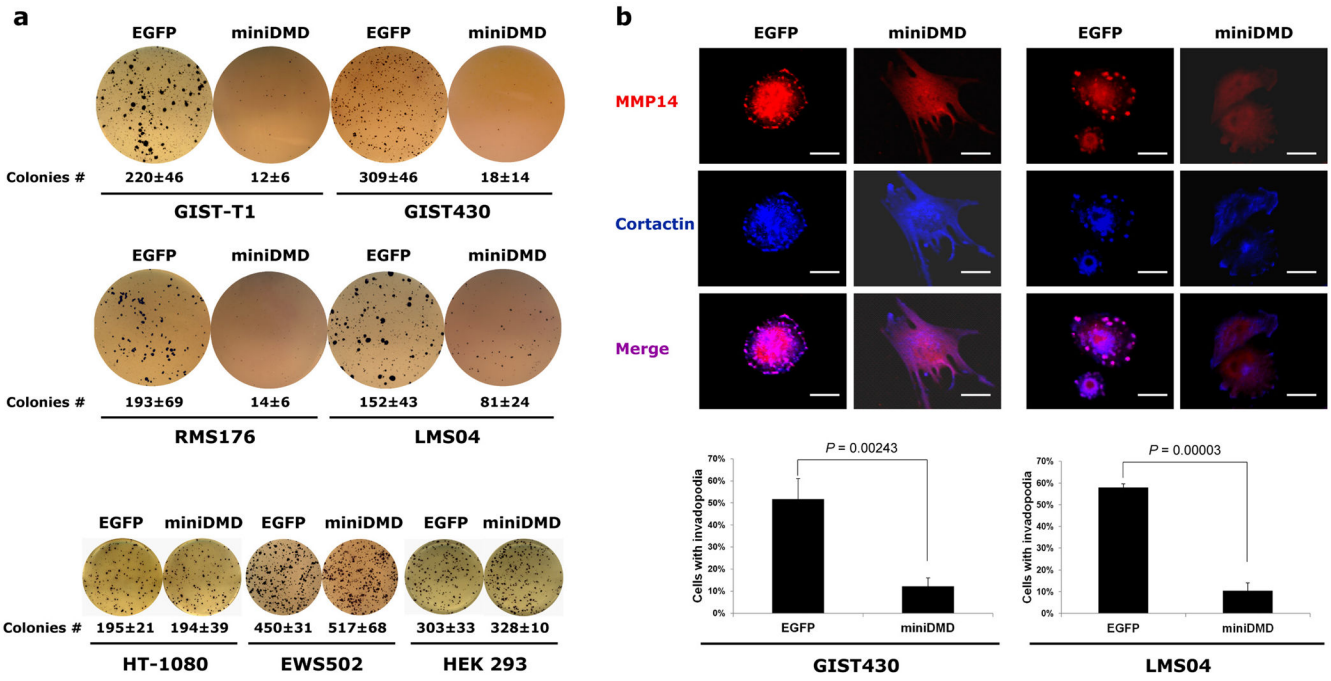

Figure 6.

Restoration of dystrophin expression inhibits anchorage-independent growth and invadopodia formation in *DMD*-inactivated myogenic cancers. Three biological replicates of each experiment were evaluated (**a**) Stable *miniDMD* expression suppresses anchorage-independent growth in myogenic cancers (GIST, RMS and LMS) but not in non-myogenic comparators (fibrosarcoma HT-1080, Ewing's sarcoma EWS502, and HEK 293) ($P<0.001$). Representative plates and mean colony numbers are shown (± standard error of the mean). (**b**) *miniDMD* restoration disrupts invadopodia formation in GIST and LMS cells. Top: Invadopodia are dot-like structures, staining with cortactin (blue) and MMP14 (red). Scale bars, 10 μm. Bottom: Percentages of cells with invadopodia in control (EGFP vector) vs. dystrophin-restoration conditions. The error bars on the histograms indicate standard deviation of the mean.